

© 2022 IEEE. Personal use of this material is permitted. Permission from IEEE must be obtained for all other uses, in any current or future media, including reprinting/republishing this material for advertising or promotional purposes, creating new collective works, for resale or redistribution to servers or lists, or reuse of any copyrighted component of this work in other works.

Cable Effects on Noise Propagation in Distribution Networks with Renewable Sources

Lu Wan, Abduselam H. Beshir, Xinglong Wu,
Xiaokang Liu, Flavia Grassi, Giordano Spadacini,
Sergio A. Pignari
Dept. of Electronics, Information and Bioengineering
Politecnico di Milano
Milan, Italy
flavia.grassi@polimi.it

Michele Zanoni,
Riccardo Chiumeo, Liliana Tenti
Ricerca sul Sistema Energetico-RSE S.p.A.
Milan, Italy
michele.zanoni@rse-web.it

Abstract—The development of power electronics for the integration of renewable energy sources in power distribution networks leads to increasing issues in terms of coexistence with communication systems, e.g., those based on powerline communications. This is due to the high-frequency noise currents, conducted emissions (CE), which, generated by power electronics devices, can propagate along the network through power cables. With the objective to provide guidelines to assure coexistence with communications systems, in this work a LV/MV distribution network is modelled and simulated in the frequency domain to predict the noise in different branches and to identify the factors that mostly affect CE propagation. The analysis mainly focuses on the effects due to power cables, and puts in evidence the need for their accurate modelling through transmission line theory in order to account for different cable features, such as per-unit-length parameters, cable length, and terminal conditions, which influence CE propagation.

Index Terms—Conducted emissions, distribution network, electromagnetic interference, transmission lines.

I. INTRODUCTION

The advanced development in power electronics has allowed the growing integration of renewable energy sources in power distribution networks, such as distributed photovoltaic (PV) systems [1], [2]. However, the high-frequency noise currents generated by these systems can interfere with communication systems within the network, such as those based on powerline communications (PLC) [3], and induce communication errors. Indeed, in recent years, several authors reported issues in smart meters due to the coexistence of power and data on the same lines [4], [5]. Hence, the development of guidelines for the design of power networks integrating renewable sources and communication systems necessarily passes through a deep understanding of how the conducted emissions (CEs) generated by the PV inverters propagate on the distribution network in a frequency range spanning from a few kilohertz (switching frequency of typical power inverters) up to several hundred kilohertz [6].

In this framework, power cables play a fundamental role in high-frequency noise propagation along the network [7].

Indeed, there are several specific issues related to conducted electromagnetic interference (EMI) in distribution networks, such as aggregation of multiple EMI sources, the influence of EMI on the performance of other devices like smart meters, and the CE propagation to the terminals of distribution networks [8]. Hence, accurate modelling of the power cables and their specific features is a key ingredient for the development of simulation tools for the prediction of noise propagation along the grid. To this end, in this paper, the high-frequency model of a simple low voltage (LV) distribution network, including loads and distributed renewable sources, is introduced and used to simulate noise propagation along the network. Specific attention is devoted to the modelling of the power cables and the LV busbar, which are represented as multi-conductor transmission lines with frequency-dependent per unit length (p.u.l.) parameters to properly account for propagation effects. In Section II, the distribution network under analysis and high-frequency models of the involved components are introduced. Specific aspects related to the modelling of power cables are addressed in the other sections, with emphasis on the effects introduced by the frequency-dependent p.u.l. parameters, line length, and different terminal connections of terminal loads.

II. MODELLING THE POWER NETWORK UNDER ANALYSIS

A. Description of the Network under Analysis

The distribution network considered in this work is shown in Fig. 1. The LV network consists of three lines (L1, L2, and L3) connected to the LV busbar, which is connected to the MV network through an L0 line and a transformer. Photovoltaic panels are connected to each branch of the power grid through inverters. Also, three-phase linear loads are considered for each branch, equipped with proper power factor correction (PFC) capacitors. The line L3 is split into two sub-branches (L3a and L3b), each of them connected to a PV panel and a linear load.

B. Component Modelling

To properly simulate the frequency response of the high-frequency noise generated by the inverters, high-frequency

This project has received funding from the European Union's Horizon 2020 research and innovation programme under the Marie Skłodowska-Curie grant agreement No 812753. This work has been partially financed by the Research Fund for the Italian Electrical System in compliance with the Decree of 16 April 2018.

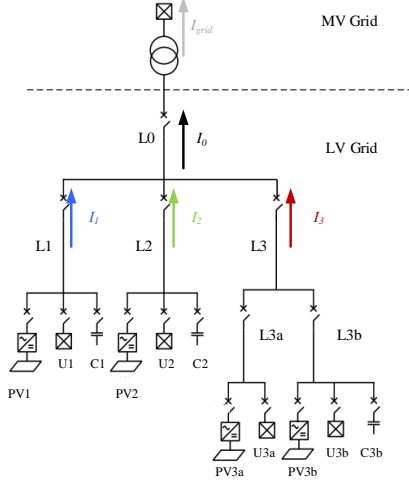


Figure 1. Single-line diagram of the LV grid under analysis.

TABLE I. Specifications of Power Cables

	Length (m)	Type	Cross-section of conductors (mm ²)	Cross-section of neutral (mm ²)
L1	80	Single-core cables with EPR* sheath	50	25
L2	70		70	35
L3a	20		25	16
L3b	30		25	16
L3	80	Three-core cables with EPR sheath and neutral cable	50	25
L0	3	Single-core cable with EPR sheath	3x70 per phase	3x35

*Ethylene Propylene Rubber

models of all components in the system, including the PV panels, the inverters, the transmission lines, the busbar, and the power transformer, are exploited. The overall model of the network is then implemented in a circuit solver (here, Ansys Circuit Design is used).

More specifically, an equivalent behavioural model is used to represent every PV unit, including the PV panels, the inverter, and the LCL filter. A detailed description of the methodology adopted to extract the parameters of such a black-box representation of the PV unit can be found in [9].

Three-phase loads are represented by equivalent RL circuits, whose parameters were evaluated starting from the nominal real and reactive powers. These data were also used to estimate theoretical capacitance values for the PFC capacitors assuring a minimum power factor equal to 0.9.

For modelling the power transformer, the behavioural model presented in [10] is adopted, whose parameters were estimated by fitting the data obtained by measurements carried out at the transformer external ports by means of proper

algorithms. The equivalent impedance of the MV network is modelled by a series RL circuit.

Though more sophisticated models rather than RL circuits for both loads and MV networks may provide more precise CE prediction, the RL circuits models used in this network greatly simplify the solution procedure, and can effectively serve the objective of this investigation, which is focused on the effects that power cables and LV busbar play on CE propagation. To properly account for propagation effects, the power lines and LV busbars are modelled by distributed-parameter circuits in accordance with transmission line (TL) theory. Accordingly, voltage and current at cable terminals are related by the chain-parameter matrix Φ [11]:

$$\begin{bmatrix} \hat{\mathbf{V}}(\mathcal{L}) \\ \hat{\mathbf{I}}(\mathcal{L}) \end{bmatrix} = \begin{bmatrix} \hat{\Phi}_{11}(\mathcal{L}) & \hat{\Phi}_{12}(\mathcal{L}) \\ \hat{\Phi}_{21}(\mathcal{L}) & \hat{\Phi}_{22}(\mathcal{L}) \end{bmatrix} \begin{bmatrix} \hat{\mathbf{V}}(0) \\ \hat{\mathbf{I}}(0) \end{bmatrix} \quad (1)$$

whose sub-matrices take the expression:

$$\begin{aligned} \hat{\Phi}_{11}(\mathcal{L}) &= \frac{1}{2} \hat{\mathbf{Y}}^{-1} \hat{\mathbf{T}}_1 (e^{\hat{\gamma}\mathcal{L}} + e^{-\hat{\gamma}\mathcal{L}}) \hat{\mathbf{T}}_1^{-1} \hat{\mathbf{Y}} \\ \hat{\Phi}_{12}(\mathcal{L}) &= -\frac{1}{2} \hat{\mathbf{Y}}^{-1} \hat{\mathbf{T}}_1 \hat{\gamma} (e^{\hat{\gamma}\mathcal{L}} - e^{-\hat{\gamma}\mathcal{L}}) \hat{\mathbf{T}}_1^{-1} \\ \hat{\Phi}_{21}(\mathcal{L}) &= -\frac{1}{2} \hat{\mathbf{T}}_1 (e^{\hat{\gamma}\mathcal{L}} - e^{-\hat{\gamma}\mathcal{L}}) \hat{\gamma}^{-1} \hat{\mathbf{T}}_1^{-1} \hat{\mathbf{Y}} \\ \hat{\Phi}_{22}(\mathcal{L}) &= \frac{1}{2} \hat{\mathbf{T}}_1 (e^{\hat{\gamma}\mathcal{L}} + e^{-\hat{\gamma}\mathcal{L}}) \hat{\mathbf{T}}_1^{-1} \end{aligned} \quad (2)$$

where: \mathcal{L} denotes the cable length, $\hat{\mathbf{T}}_1$ is a similarity transformation matrix diagonalizing the matrix product $\hat{\gamma}^2 = \hat{\mathbf{T}}_1^{-1} \hat{\mathbf{Y}} \hat{\mathbf{Z}} \hat{\mathbf{T}}_1$, $\hat{\mathbf{Y}}, \hat{\mathbf{Z}}$ denote the p.u.l. admittance and impedance matrices, respectively, and is the diagonal matrix containing the line propagation constants [11]. These parameters are inherently related to the specific conductor arrangement in the cable cross-section, which is hereinafter assumed to be constant over the line length so as to adopt a uniform TL model.

To improve the computational efficiency of parametric simulation (for instance, the parameter sweep of cable length in Section IV), a Matlab routine is created specifically for the network under analysis and verified by the Ansys model. In the routine, each component (excluding the loads connected to the terminations) is modelled in terms of a 2N-port network (with N=4) and characterized by means of appropriate chain parameters.

Besides, it is important to note that TL p.u.l. parameters are functions of the operating frequency, mainly owing to the skin effect which causes a progressive increase of the p.u.l. resistance and, at the same time, a progressive decrease of the internal p.u.l. inductance of the conductor. The influence of the frequency-dependence of TL p.u.l. parameters on noise propagation will be investigated in Section III.

C. CE Prediction under Nominal Conditions

To predict the CEs propagation in the LV grid under analysis (see Fig. 1 and cable specifications in Tab. 1.), frequency-domain simulations are carried out by exploiting

the Matlab routine in the frequency range from 2 kHz up to 1 MHz (10 Hz frequency resolution). The spectra of the noise currents of phase U propagating from branches L1, L2, L3 to the busbar (i.e., currents I_1 , I_2 , and I_3) are compared with the spectra of the total noise current before (i.e., current I_0 in Fig. 1) and after (i.e., current I_{grid} in Fig. 1) the power transformer in Fig. 2(a). To simplify the comparison, Fig. 2(b) shows the peak envelopes of previous spectra, which are obtained by the Matlab *findpeaks* function with the minimum separation of peaks set to 4 kHz.

The comparison shows that the amplitude of the total noise current I_0 is higher than the amplitude of the other currents I_1 , I_2 , and I_3 for frequencies lower than (approximately) 300 kHz. This is no (necessarily) longer true at higher frequencies, where the amplitude of I_0 is comparable with others. This result is explained by the fact that currents I_1 , I_2 , and I_3 have different phases, and therefore, the aggregation may be either additive or subtractive. For the specific network configuration under analysis, the aggregation is mainly additive below 300 kHz and subtractive at a higher frequency. Besides, comparing the contribution in LV branches, the noise current in branch L3 exhibits a significantly higher amplitude than those in the other two branches, whose amplitudes, instead, are comparable. Moreover, the current on the MV side (current I_{grid}) results to be significantly attenuated with respect to the current on the LV side of branch L0 (current I_0), showing that power transformers can effectively filter out the high-frequency noise coming from the LV network.

III. P.U.L. PARAMETERS FREQUENCY DEPENDENCE

This Section investigates the influence of the frequency-dependence of the TL p.u.l. parameters on noise propagation. To this end, the simplified setup in Fig. 3 is considered, which only involves the 500-meter cable L3, the corresponding load (equipped with PFC capacitors) and the PV unit. The line is terminated in a three-phase Line Impedance Stabilization Network (LISN), as prescribed by International Standards for CE measurement. Simulations are carried out in the Ansys Circuit toolbox by means of four different sets of p.u.l. parameters. In the first three cases, constant p.u.l. parameters numerically evaluated at 50 Hz, 2 kHz, and 1 MHz are used. In the fourth case, hereinafter considered as the reference solution, the p.u.l. parameters were numerically evaluated frequency-by-frequency (with 10 Hz resolution) in the interval from 2 kHz to 1 MHz.

The obtained CE spectra are compared in Fig. 4. The comparison reveals significant differences in the whole frequency interval when constant p.u.l. parameters evaluated at 50 Hz are used, see Fig. 4(a). These differences are limited to high frequency in the spectra shown in Fig. 4(b), and definitely less evident in Fig. 4(c). These results are mainly of interest for time-domain simulation, where the implementation of frequency-dependent p.u.l. parameters is often unfeasible and/or may lead to causality or convergence issues. Namely, the simulations prove the possibility to resort to constant p.u.l. parameters, on condition they were evaluated at a suitable frequency. As shown in Fig. 4(c), the use of p.u.l. parameters

evaluated at 1 MHz allows for obtaining accurate CE predictions in the frequency range of interest (2 kHz - 1 MHz).

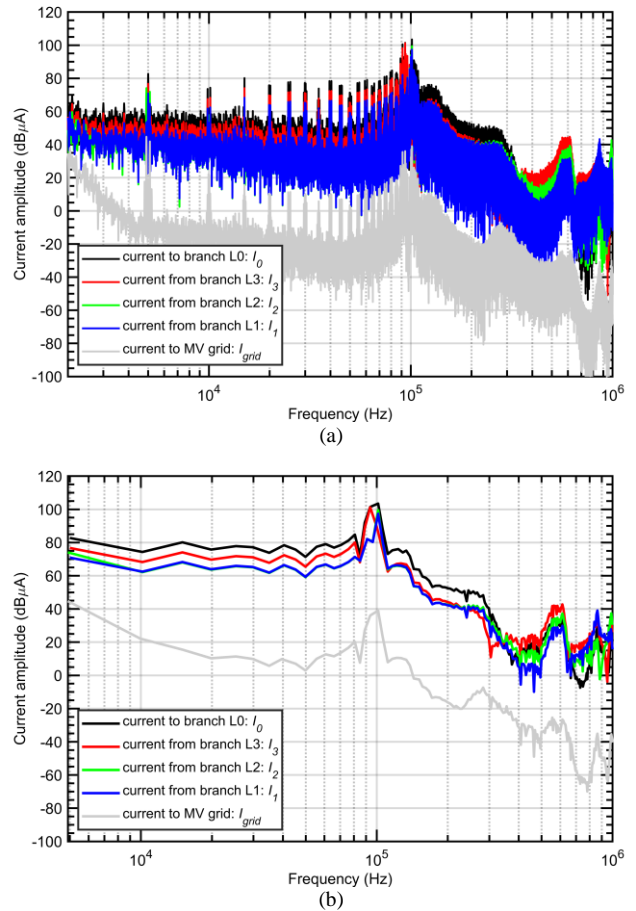


Figure 2. Noise currents on different lines (see Fig. 1): (a) Frequency spectra and (b) peak envelopes.

IV. EFFECTS DUE TO CABLE LENGTH

In this section, the influence of the length of individual cables on the overall emission levels is analyzed. To this end, the original network in Fig. 1 is considered, and the length of cable L3 is varied from 1 m up to 500 m. Parametric simulations are carried out by the Matlab routine.

Fig. 5(a) compares the spectra of the current of phase U flowing from the busbar to branch L0 for four different lengths of cable L3. The comparison in terms of voltages of phase U at the busbar is presented in Fig. 5(b). The comparisons show that at low frequencies (below around 30 kHz), there are no significant differences in the emission levels. The high-frequency behaviour is more complex. In general, all spectra show similar noise levels, with peaks occurring at different frequencies. Indeed, in line with TL theory, resonance peaks shift towards lower frequencies as the cable length increases due to propagation effects.

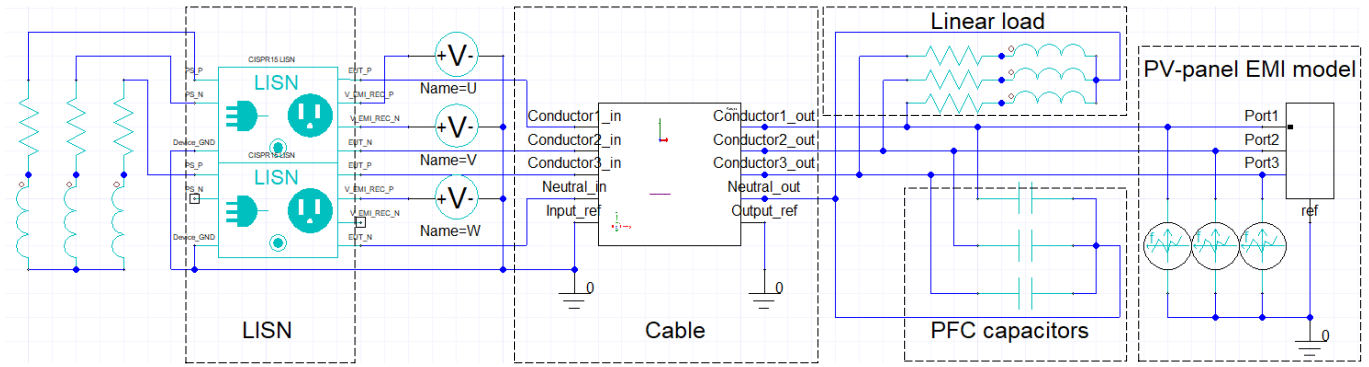


Figure 3. Simplified test setup involving a single branch of the LV network in Fig. 1, the corresponding load and PFC capacitors and the PV unit.

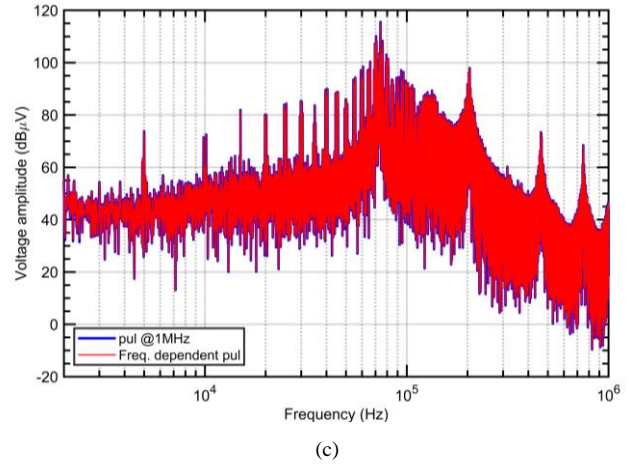
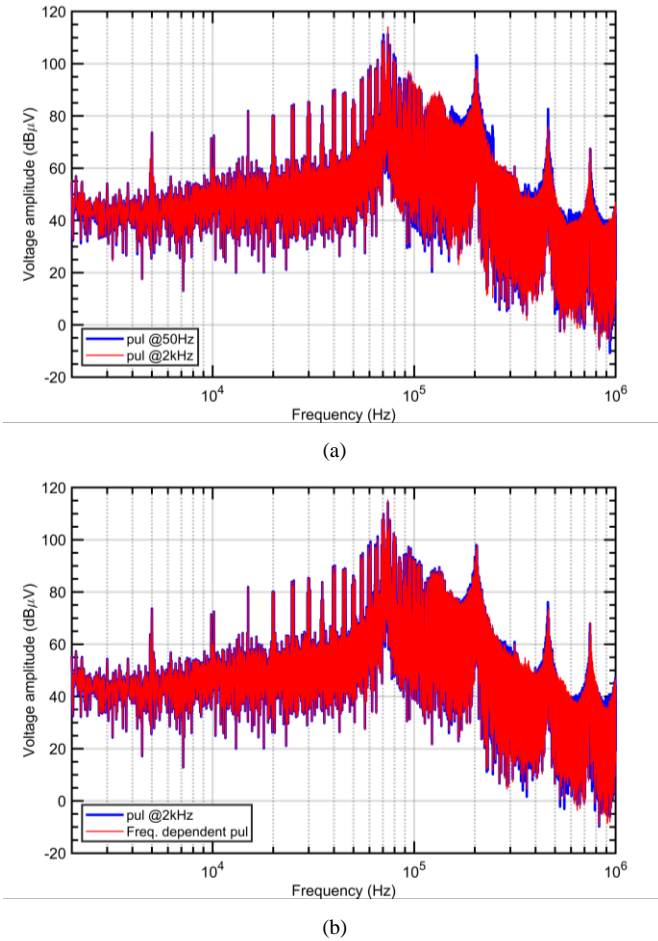


Figure 4. Prediction of the voltages at the LISN ports (phase U), see Fig. 3, for different p.u.l. parameters of cable L3: (a) Constant p.u.l. parameters evaluated at 50 Hz and 2 kHz; (b) constant p.u.l. parameters evaluated at 2 kHz v.s. f-dependent parameters; and (c) simulations with constant parameters evaluated at 1 MHz v.s. f-dependent parameters.

V. EFFECTS DUE TO THE POWER FACTOR CORRECTION CAPACITORS

In this section, the impact of power-factor correction capacitors in the emissions propagation along the power line is investigated by the Matlab routine (see Fig. 6) as described in (1). In both cases, the three-phase loads are star-connected, as well as their corresponding power factor capacitors. However, in the first case, their star point is connected to the neutral, Fig. 6 (a). In the second case, it is left floating, Fig.6 (b).

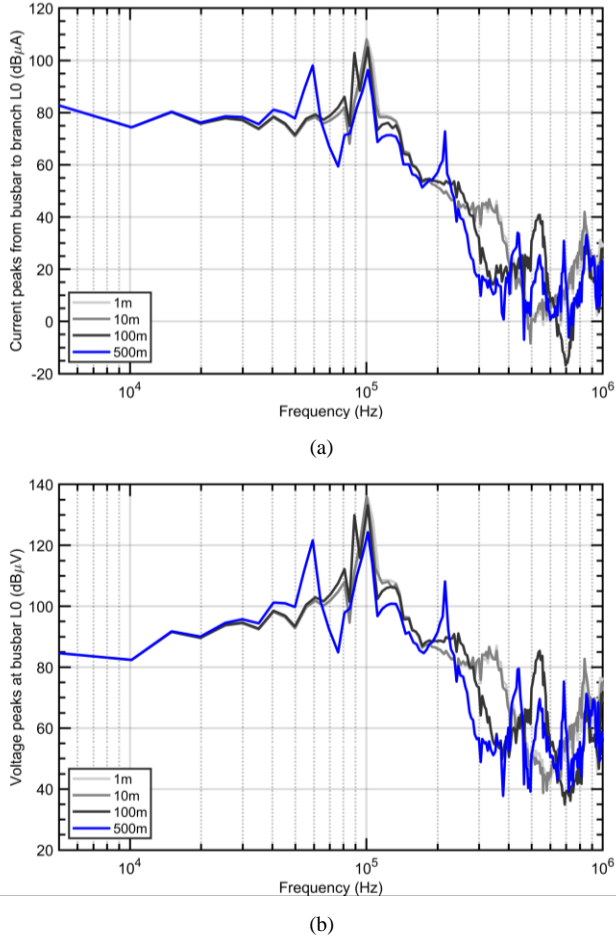


Figure 5. CE prediction for different lengths of cable L3: (a) current of phase U from the LV busbar to branch L0, and (b) voltage of phase U at the intersection between the LV busbar and branch L0.

The comparison in Fig. 7(a) shows appreciable larger emissions over the entire frequency range when the star point is floating. To investigate further this aspect, the three-phase currents (phase U, V, W) are decomposed into zero, direct (positive) and inverse (negative) sequence currents by

$$\begin{bmatrix} I_{zero} \\ I_{direct} \\ I_{inverse} \end{bmatrix} = \frac{1}{3} \begin{bmatrix} 1 & 1 & 1 \\ 1 & e^{j2\pi/3} & e^{j4\pi/3} \\ 1 & e^{j4\pi/3} & e^{j2\pi/3} \end{bmatrix} \begin{bmatrix} I_U \\ I_V \\ I_W \end{bmatrix} \quad (3)$$

and compared separately. The results obtained for the zero-sequence current allow ascribing the observed reduction to a significant reduction of the zero-sequence component, which is the dominant contribution to the overall phase current, when the neutral is connected to the star point of the three-phase loads and power factor correction capacitors. It is worth mentioning, however, that this reduction is not as large as it could be expected. As a matter of fact, since the neutral is grounded at the LV side of the transformer only, in the frequency range of interest, the actual impedance between the neutral and ground results to be quite large (due to the presence of the cables) thus significantly reducing the expected beneficial effect of noise reduction played by the power-factor correction capacitors.

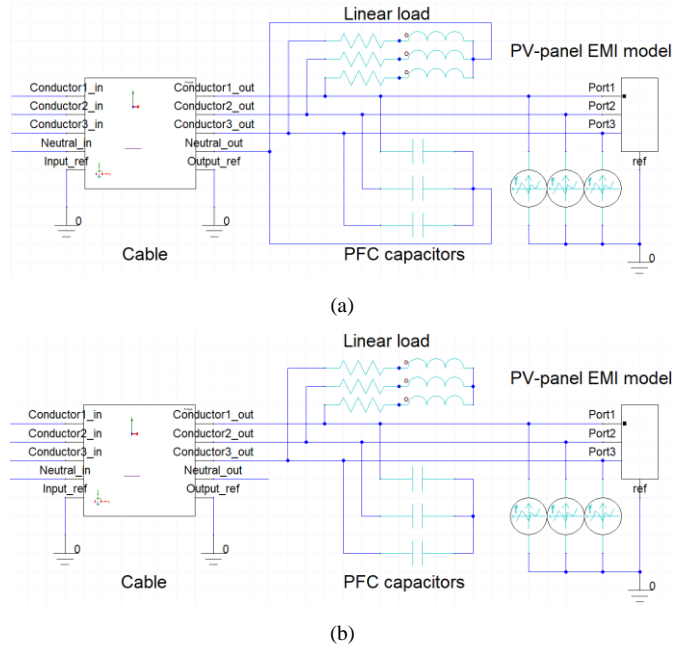


Figure 6. Different terminal connections of loads at the LV network: (a) the star points of loads and PFC capacitors are connected to the neutral cable, and (b) the star points of loads and PFC capacitors are floating.

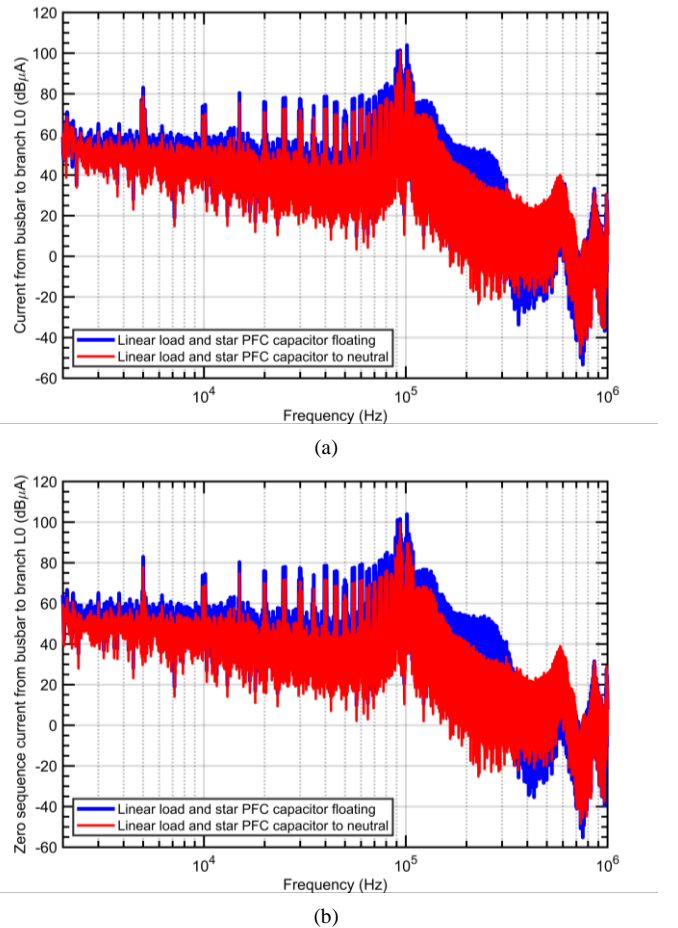


Figure 7. CE predictions of current from the LV busbar to branch L0: (a) current of phase U, (b) zero-sequence current.

VI. CONCLUSIONS

In this work, the propagation of the CEs generated by the inverters used to interface distributed PV units with a LV power network has been investigated by resorting to frequency-domain simulations in the interval from 2 kHz up to 1 MHz. To this end, a simple LV distribution network has been modelled, by implementing high-frequency models of the involved components.

The analysis was aimed at putting in evidence the need for accurate modelling of the cables, as they play a fundamental role in noise propagation. To this end, all power cables and the LV busbar were modelled as multi-conductor transmission lines, whose p.u.l. parameters were numerically evaluated. Particularly, two main influence factors were put in evidence, that is: the impact of the cable length as well as the influence of different terminal conditions.

Moreover, the analysis allows appreciating the need for careful evaluation of the involved p.u.l. parameters, whose frequency dependence, if not correctly accounted for, may jeopardize the accuracy of CE prediction in the frequency interval of interest.

ACKNOWLEDGMENT

This project has received funding from the European Union's Horizon 2020 research and innovation programme under the Marie Skłodowska-Curie grant agreement No 812753. This work has been partially financed by the Research Fund for the Italian Electrical System in compliance with the Decree of 16 April 2018.

REFERENCES

- [1] M. Hashmi, S. Hanninen, and K. Maki, "Survey of smart grid concepts, architectures, and technological demonstrations worldwide," in *2011 IEEE PES Conference on Innovative Smart Grid Technologies (ISGT Latin America)*, Medellin, Colombia, Oct. 2011, pp. 1–7. doi: 10.1109/ISGT-LA.2011.6083192.
- [2] I. Colak, E. Kabalci, G. Fulli, and S. Lazarou, "A survey on the contributions of power electronics to smart grid systems," *Renewable and Sustainable Energy Reviews*, vol. 47, pp. 562–579, Jul. 2015, doi: 10.1016/j.rser.2015.03.031.
- [3] A. E. Shadare, M. N. O. Sadiku, and S. M. Musa, "Electromagnetic compatibility issues in critical smart grid infrastructure," *IEEE Electromagn. Compat. Mag.*, vol. 6, no. 4, pp. 63–70, 2017, doi: 10.1109/MEMC.0.8272283.
- [4] P. Kotsampopoulos *et al.*, "EMC Issues in the Interaction Between Smart Meters and Power-Electronic Interfaces," *IEEE Trans. Power Delivery*, vol. 32, no. 2, pp. 822–831, Apr. 2017, doi: 10.1109/TPWRD.2016.2561238.
- [5] F. Leferink, C. Keyer, and A. Melentjev, "Static energy meter errors caused by conducted electromagnetic interference," *IEEE Electromagn. Compat. Mag.*, vol. 5, no. 4, pp. 49–55, 2016, doi: 10.1109/MEMC.2016.7866234.
- [6] A. Abart and G. F. Bartak, "EMI of emissions in the frequency range 2 kHz - 150 kHz," in *22nd International Conference and Exhibition on Electricity Distribution (CIRED 2013)*, Stockholm, Sweden, 2013, pp. 1271–1271. doi: 10.1049/cp.2013.1151.
- [7] S. A. Pignari and A. Orlandi, "Long-cable effects on conducted emissions levels," *IEEE Trans. Electromagn. Compat.*, vol. 45, no. 1, pp. 43–54, Feb. 2003, doi: 10.1109/TEMC.2002.808023.
- [8] L. Chhaya, P. Sharma, A. Kumar, and G. Bhagwatikar, "EMI Concerns, Measurements and Standards for Smart Grid," in *Advances in Greener Energy Technologies*, A. K. Bhoi, K. S. Sherpa, A. Kalam, and G.-S. Chae, Eds. Singapore: Springer Singapore, 2020, pp. 123–136. doi: 10.1007/978-981-15-4246-6_6.
- [9] L. Wan *et al.*, "Black-Box Modelling of Low-Switching-Frequency Power Inverters for EMC Analyses in Renewable Power Systems," *Energies*, vol. 14, no. 12, p. 3413, Jun. 2021, doi: 10.3390/en14123413.
- [10] M. Bigdeli, M. Valii, and D. Azizian, "Applying Intelligent Optimization Algorithms for Evaluation of Transformer Black Box Model," in *Soft Computing Applications*, vol. 357, V. E. Balas, L. C. Jain, and B. Kovačević, Eds. Cham: Springer International Publishing, 2016, pp. 1271–1286. doi: 10.1007/978-3-319-18416-6_102.
- [11] C. R. Paul, *Analysis of multiconductor transmission lines*, 2nd ed. Hoboken, N.J: Wiley-Interscience : IEEE Press, 2008.